Am J Transl Res 2020;12(12):7908-7922
www.ajtr.org /ISSN:1943-8141/AJTR0112569

Original Article

iTRAQ quantitative proteomic analysis differentially expressed proteins and signal pathways in henoch-schönlein purpura nephritis

Ran Gao[1], Xueli Niu[2], Lili Zhu[3], Ruiqun Qi[2], Liang He[4]

[1]Department of Hematology, No. 1 Hospital of China Medical University, Shenyang 110001, Liaoning, China; [2]Department of Dermatology, No. 1 Hospital of China Medical University and Key Laboratory of Immunodermatology, Ministry of Health and Ministry of Education, Shenyang 110001, Liaoning, China; [3]Department of Dermatology, The People's Hospital of China Medical University and The People's Hospital of Liaoning Province, Shenyang 110016, Liaoning, China; [4]Department of Thyroid Surgery, No. 1 Hospital of China Medical University, Shenyang 110001, Liaoning, China

Received April 14, 2020; Accepted November 3, 2020; Epub December 15, 2020; Published December 30, 2020

Abstract: Henoch-Schönlein purpura nephritis (HSPN) has been considered as a major cause of chronic renal failure in children and a condition which can worsen clinical outcomes in adults. At present, the molecular mechanisms of HSPN are still unclear. In this study, iTRAQ quantitative proteomic analysis was performed on renal tissues collected from patients with HSPN and compared with those of patients after nephrectomy (controls). A total of 149 differentially expressed proteins (DEPs) were detected, of which, 97 being upregulated and 52 down-regulated. Protein functions and classifications were analyzed using Gene ontology (GO) and Kyoto Encyclopedia of Genes and Genomes (KEGG). In addition, protein domains. expressive hierarchical clustering analysis and protein-protein interaction (PPI) analysis were also conducted for DEPs. The results of bioinformatics analysis indicated that DEPs were enriched in lipid metabolism and the adherens junction pathway. Among these proteins, CDC42 and CTNNB1 were identified as potential candidates involved in the pathogenesis of HSPN. Immunohistochemistry and real-time PCR further demonstrated that CDC42 and CTNNB1 were up-regulated in HSPN patients. These results provide new and important insights into some underlying molecular pathogenesis of HSPN.

Keywords: Henoch-schönlein purpura nephritis, bioinformatic analysis, lipid metabolism, cytoskeleton, molecular mechanism

Introduction

Henoch-Schönlein purpura (HSP) is a systemic vasculitis demonstrated by IgA deposits. This condition affects small vessels of the joints, kidneys, gastrointestinal tract and skin [1, 2]. Although HSP is typically self-limiting and its prognosis is largely favorable, kidneys may be involved, which can aggravate the severity of this disease. As a result, permanent organ damage in the form of severe HSP nephritis (HSPN) may ensue, thus the renal involvement of the disease can be used as the main prognostic factor [3]. It is considered that HSPN is more prevalent in the pediatric population, and the proportion of all children with HSP progressing to HSPN is approximately 30-50% [4, 5]. HSP is less common in adults, but it is often associated with more severe clinical manifestations and renal outcomes, and an estimated risk of progression of HSP to chronic renal insufficiency is 25-30% [6, 7].

Based on the results from a number of clinical and experimental studies, it appears that the deposition of IgA-containing immune complexes, which leads to the renal damage and inflammatory, changes in other organs in HSPN patients [8]. Actually, numerous pro-inflammatory cytokines are expressed in HSPN following immune complex deposition [9]. Therefore, complex biomolecular mechanisms activated in response to IgA deposition may also exert an important effect in the pathogenesis of HSPN.

However, the pathogenesis of HSPN remains largely unknown, a number of factors that can produce HSP have been identified, including genetic factors, bacterial or viral infections and environmental influences [10].

A relatively novel approach to explore the pathogenesis of diseases involves use of quantitative proteomics. With this technique it is possible to identify and compare quantitatively unique proteins within biological samples [11]. The proteomic technique is increasingly used in kidney disease [3, 12, 13], but it is quite rarely used in studies focusing on HSPN. In this current study, renal tissue samples from HSPN patients were analyzed using iTRAQ quantitative proteomic analysis and compared with those from the patients after nephrectomy who served as controls. Such an analysis can provide plenty of information on pathogenic mechanisms of HSPN, as well as an understanding of the complex biological processes activated in response to HSP.

Materials and methods

Sampling and pathological diagnosis

Fresh renal tissue was harvested from 5 HSPN patients undergoing kidney puncture biopsy including 3 males and 2 females, with an age range of (20-40) years. Renal tissues serving as controls were harvested from 4 patients after nephrectomy due to abdominal trauma. The controls consisted of 2 males and 2 females with an age range of (20-40) years and their pathological diagnoses of HSPN were confirmed by pathologists from No. 1 Hospital of China Medical University. Six renal tissue samples (3 patients and 3 controls) were subjected to protein extraction for iTRAQ proteomics analysis. All renal tissue samples were prepared for paraffin embedding and mRNA extraction, and renal samples were also prepared for iTRAQ quantification. For hematoxylin and eosin (HE, Solarbio, China) staining, a microtome was used to prepare paraffin-embedded tissues sections (5 μm thickness) and then HE staining was performed.

iTRAQ quantitative proteomics analysis

Renal tissue samples of the patients were used to iTRAQ quantitative proteomics assay. This part of work was commissioned by a technical service company (PTM Biolab, Hangzhou, China). The experiments included protein extraction, isobaric labeling, HPLC fractionation and mass spectrometry-based quantitative proteomic analysis. Bioinformatic analysis was then performed to investigate quantifiable targets, including protein annotation, functional classification, functional enrichment, subcellular localization, and cluster analysis based on functional enrichment.

Immunohistochemistry

Paraffin sections of renal samples were deparaffinized, rehydrated and repaired antigen using citrate buffer solution. The sections were blocked in 10% goat serum and then cultured overnight at 4°C using anti-human β-catenin or anti-human CDC42 antibodies (Abcam, UK). Subsequently the sections were cultured using the secondary antibody, and HE staining were performed using EliVision Super Kit (Maixin, China). The sections were photographed using a Nikon Eclipse Ti microscope.

Real-time PCR

Fresh renal tissues were collected from HSPN patients and healthy controls, respectively. miRNeasy Mini Kit (Qiagen, Germany) was used to extract the mRNAs of all samples. cDNAs were synthesized by using the mRNA (1 μg) as a template. Primer sequence (GAPDH: sense 5'-AAGAGCACAAGAGGAAGAGAGAGAC-3', antisense 5'-GTCTACATGGCAACTGTGAGGAG-3'; CTNNB1; sense 5'-ACCAGTGGATTCTGTGTTG-3', anti-sense 5'-AAGGCAGTCTGTCGTAATAG-3'; CDC42: sense 5'-GATTACGACCGCTGAGTTA-3'; anti-sense 5'-CTGGAGTGATAGGCTTCTG-3'). The expression levels of mRNA were detected by 7900HT Fast Real-Time PCR System (Applied Biosystems, USA) using RT2 SYBR Green qPCR Master mix (Promega, USA).

Statistical analyses

A statistical software (version 20.0, IBM, USA) was used to perform statistical analyses. The data were presented as the mean ± SD. The statistical significance of the differences between groups was assessed using Fisher's exact test $P < 0.05$ indicated that the difference was as statistically significant.

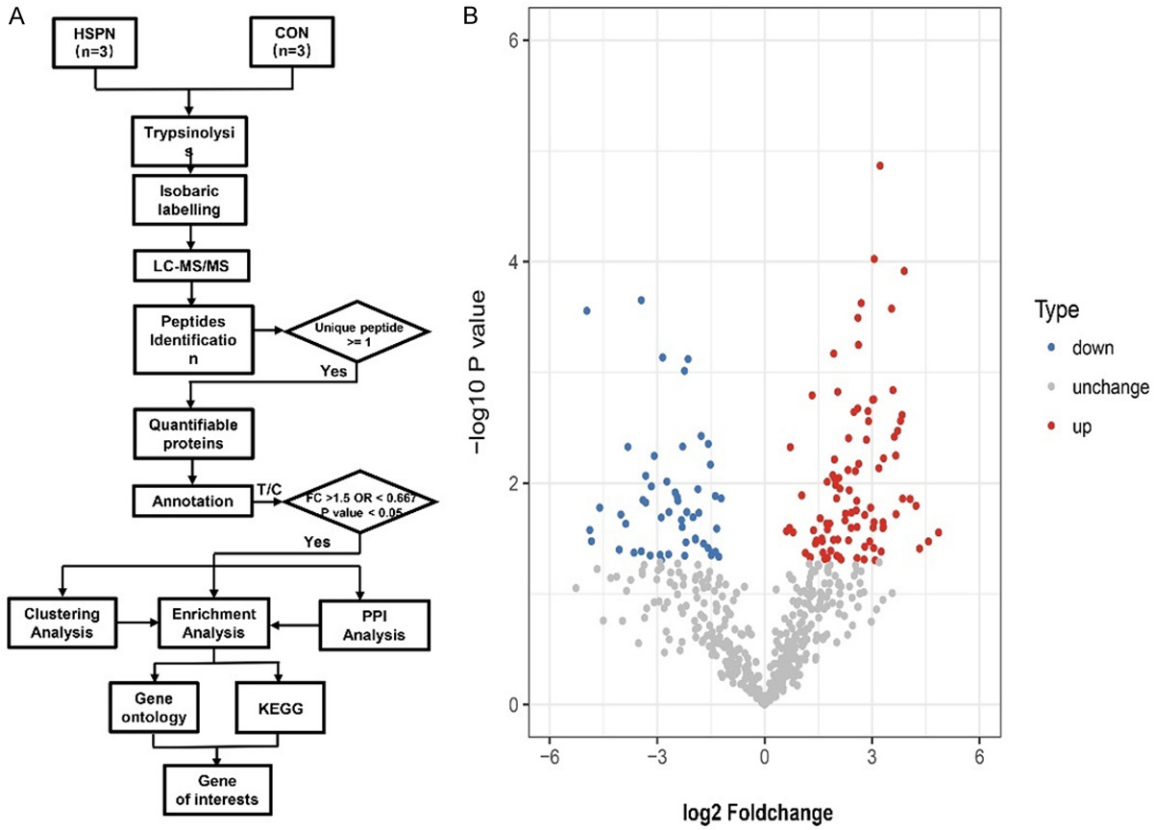

Figure 1. Workflow diagram and Volcano Plot for protein expressions. A. Summary of procedures involved with sample preparation, grouping, iTRAQ labeling, MS detection and bioinformatics analysis used in this study. B. Volcano plot for identifying proteins. Red spots indicate significantly up-regulated protein expressions blue spots indicate down-regulated protein expressions and grey spots indicate an absence of statistically significant differences in protein expressions. The greater the ordinate value corresponding to the point, the greater the corresponding difference in protein expression. Similarly, the greater the absolute value of the abscissa corresponding to the point, the greater the corresponding difference in protein expression. There were 149 statistically significant DEPs identified with up-regulated DEPs having an abscissa value of > 1.5 and down-regulated DEPs an abscissa value of < 0.667.

Results

Identification of differentially expressed proteins in renal tissue of normal versus HSPN patients

iTRAQ-based quantitative proteomic analysis of renal tissues from normal and HSPN patients was performed according to the procedure shown in **Figure 1A**, so as to detect potential protein alterations in response to HSPN. According to the above-mentioned criteria [14], a total of 814 proteins were detected, among which 571 were quantified. As screened using a 1.5 fold cutoff criterion (HSPN group/control group > 1.5 or < 0.667) combined with a significant Fisher's exact test *P*-value, 149 proteins were determined as differentially expressed proteins (DEPs), of which, 97 DEPs were up-regulated and 52 DEPs down-regulated (**Figure 1B**).

Subcellular structural localization

Subcellular localization revealed that the up-regulated DEPs were mainly located within the cytoplasm (38%) and mitochondria (26%), and only 5% of up-regulated DEPs were distributed in the nucleus. The down-regulated DEPs were mostly located in the nucleus (43%) and cytoplasm (29%), and only 10% of down-regulated DEPs were located in the mitochondria (**Figure 2**).

GO and KEGG pathway enrichment analysis

To further disclose the biological functions of these 149 DEPs, GO enrichment was analyzed

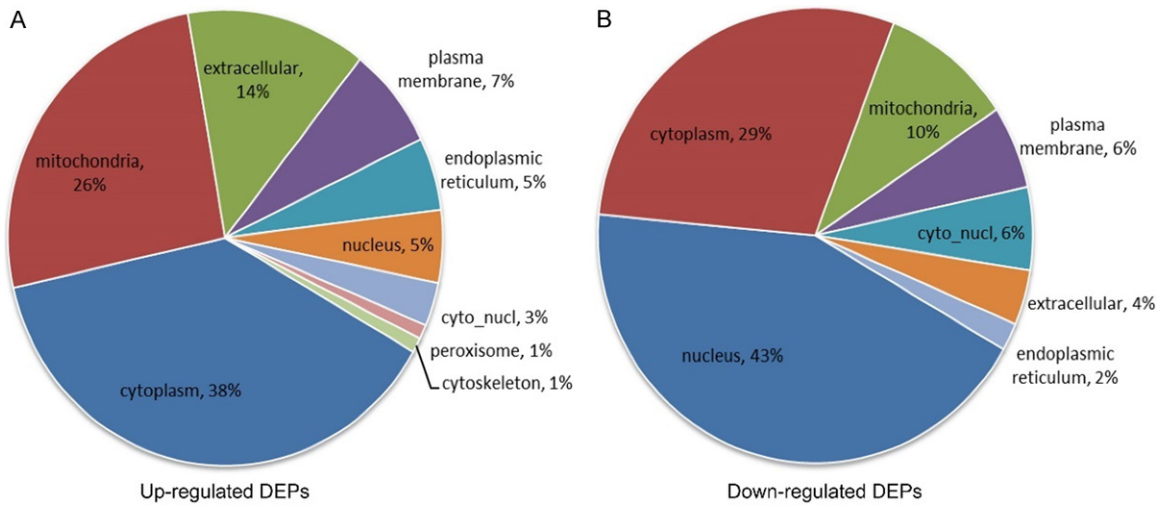

Figure 2. Sub-cellular location analysis. A. Up-regulated DEPs were mainly distributed within the cytoplasm (38%) and mitochondria (26%) and only 5% in the nucleus. B. Down-regulated DEPs were mainly distributed within the nucleus (43%) and cytoplasm (29%) and only 10% in the mitochondria.

using InterProScan software. Biological process (BP), molecular function (MF) and cellular component (CC) were sorted by protein count and visual information of the three GO categories are summarized in **Figure 3**. In addition, detailed information on the up- or down-regulated DEPs in the three GO categories were listed in **Tables 1** and **2**.

In the biological process function group, up-regulated DEPs were mainly enriched in the single organism metabolic process, especially in organic acid, while down-regulated DEPs were mainly enriched in dephosphorylation regulation and organelle organization. With regard to cellular component enrichment analyses, up-regulated DEPs were mainly located in mitochondria, while down-regulated DEPs were contained in cytoskeletal proteins and cell projection part. In the molecular function enrichment group, up-regulated DEPs were mainly related to co-factor binding, acetyltransferase activity and co-enzyme binding. However, down-regulated DEPs were enriched in guanyl-nucleotide exchange factor activity, cytoskeleton binding and calmodulin binding.

KEGG database was used to conduct KEGG enrichment analysis on these DEPs. The vascular smooth muscle contraction pathway was only present in the group with down-regulated DEPs (**Table 3**). In the group with up-regulated DEPs, signaling pathways were mainly enriched in metabolic pathways of butanoate, alanine, amino sugars and nucleotide sugars as well as in adherens junction (**Figure 3C**).

Protein domain enrichment

To examine the domain function of DEPs, up- and down-regulated DEPs were subjected to enrichment analyses of protein domains. The results revealed that down-regulated proteins mainly contained the EF-hand domain, SH3 domain and C-terminal and Band4.1. By contrast, up-regulated proteins mainly contained the SGNH hydrolase-type esterase domain, aminoacyl-tRNA synthetase (class II) and thiamin diphosphate-binding fold (**Figure 3D**).

Functional enrichment-based hierarchical clustering analysis of the DEPs

To further understand the function of these DEPs in HSPN patients, hierarchical clustering analysis was performed to evaluate the functional relationships between them. In the biological process category, up-regulated proteins were mainly enriched in multiple lipid metabolism, positive regulation of cell growth and coenzyme biosynthetic process (**Figure 4A**), while down-regulated proteins were mainly implicated in the regulating cell morphogenesis, GTPase activity and biosynthetic processes. In addition, it was found that down-regulated proteins were also highly enriched during

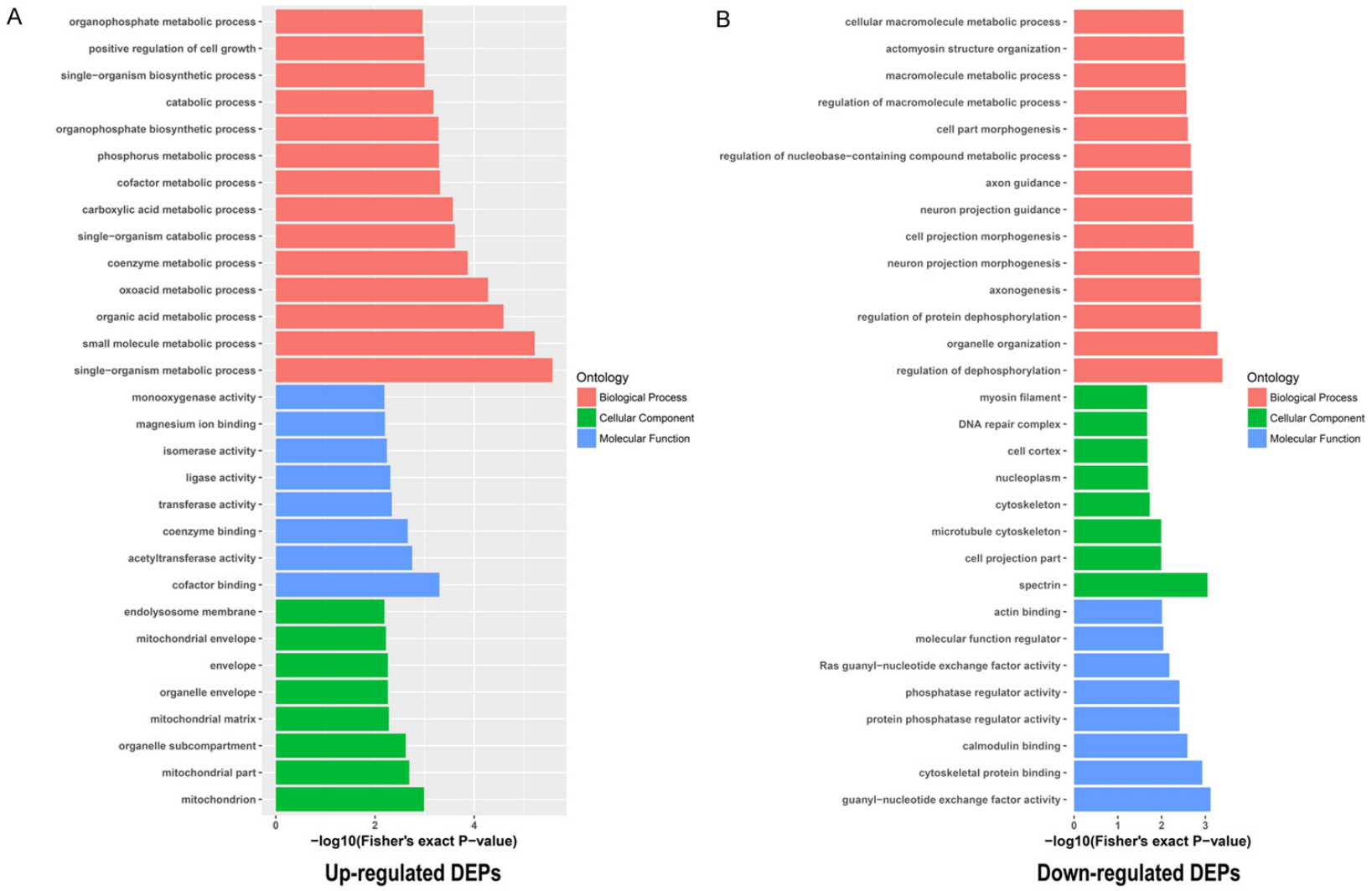
A
organophosphate metabolic process
positive regulation of cell growth
single−organism biosynthetic process
catabolic process
organophosphate biosynthetic process
phosphorus metabolic process
cofactor metabolic process
carboxylic acid metabolic process
single−organism catabolic process
coenzyme metabolic process
oxoacid metabolic process
organic acid metabolic process
small molecule metabolic process
single−organism metabolic process
monooxygenase activity
magnesium ion binding
isomerase activity
ligase activity
transferase activity
coenzyme binding
acetyltransferase activity
cofactor binding
endolysosome membrane
mitochondrial envelope
envelope
organelle envelope
mitochondrial matrix
organelle subcompartment
mitochondrial part
mitochondrion
0
2
4
−log10(Fisher's exact P−value)
Up-regulated DEPs
Ontology
Biological Process
Cellular Component
Molecular Function
B
cellular macromolecule metabolic process
actomyosin structure organization
macromolecule metabolic process
regulation of macromolecule metabolic process
cell part morphogenesis
regulation of nucleobase−containing compound metabolic process
axon guidance
neuron projection guidance
cell projection morphogenesis
neuron projection morphogenesis
axonogenesis
regulation of protein dephosphorylation
organelle organization
regulation of dephosphorylation
myosin filament
DNA repair complex
cell cortex
nucleoplasm
cytoskeleton
microtubule cytoskeleton
cell projection part
spectrin
actin binding
molecular function regulator
Ras guanyl−nucleotide exchange factor activity
phosphatase regulator activity
protein phosphatase regulator activity
calmodulin binding
cytoskeletal protein binding
guanyl−nucleotide exchange factor activity
0
1
2
3
−log10(Fisher's exact P−value)
Down-regulated DEPs
Ontology
Biological Process
Cellular Component
Molecular Function

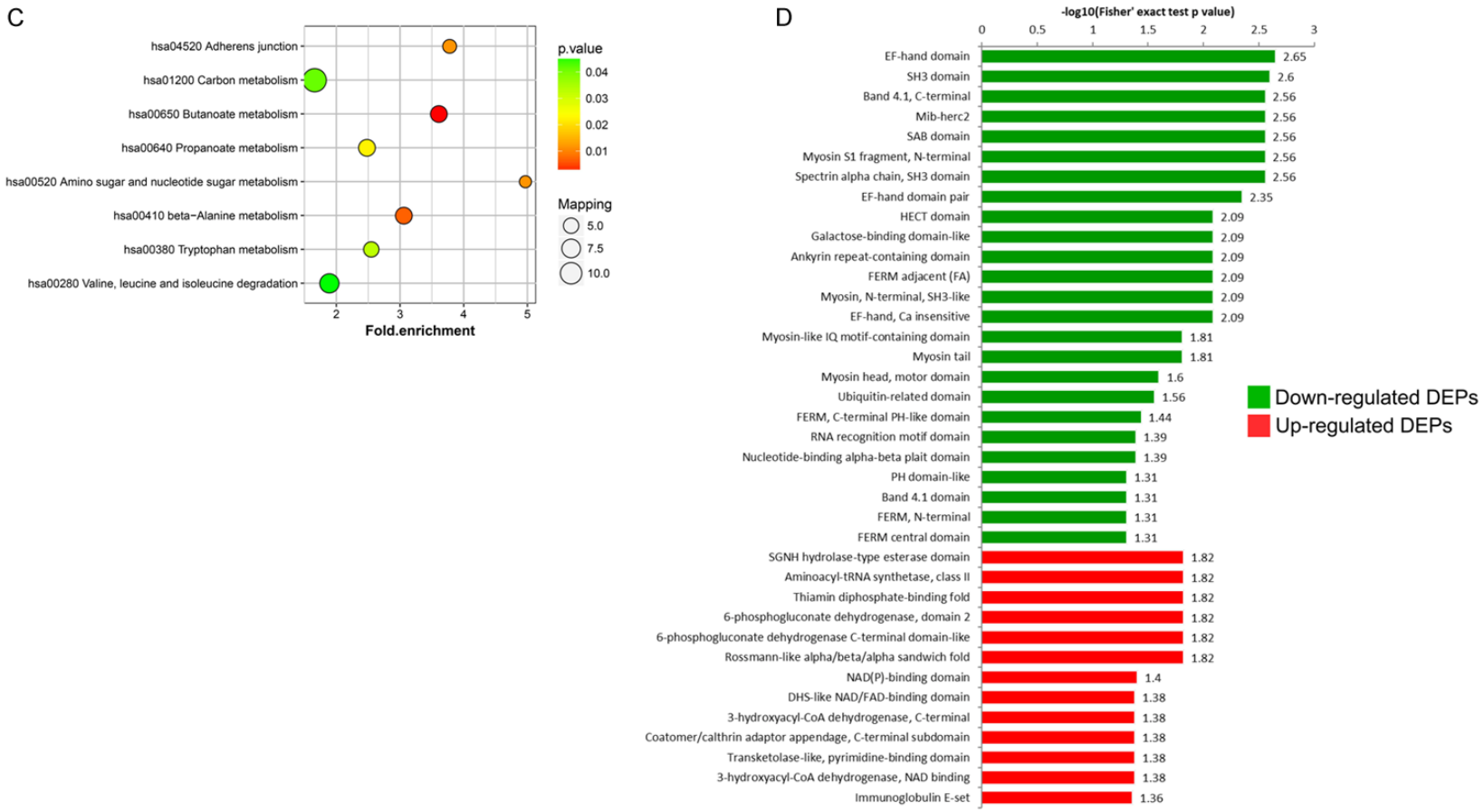

Figure 3. Functional analysis of DEPs. (A) GO enrichment of up-regulated DEPs in 3 functional groups: biological processes (red bar), cellular components (green bar) or molecular functions (blue bar). (B) GO enrichment of down-regulated DEPs. (C) KEGG enrichment analysis of up-regulated DEPs. The colored circle indicates significant differences in DEPs and *p* value within each KEGG pathway. The degree of enrichment of the signaling pathway is denoted by the color circle, with red indicating greater degrees of enrichment while green less enrichment. The fold of enrichment is presented as the ratio (%) of the number of DEPs annotated in a pathway (as indicated in the y-axis) to the number of all proteins annotated in this pathway. (D) Protein domain enrichment analysis. The abscissa value corresponds to the length of the bar plots (-log10; Fisher's exact *P*-value), with the greater the bar plot length the greater the enrichment degree of DEPs (A, B and D). DEPs, differently expressed proteins; GO, gene ontology; KEGG, Kyoto Encyclopedia of Genes and Genomes.

Table 1. GO analysis of up-regulated proteins associated with HSPN

Term	Count	Fold enrichment	Fisher' exact test *P* value	-log10 (*p* value)	Function
GO:0044710 single-organism metabolic process	59	1.56	2.62E-06	5.58	BP
GO:0044281 small molecule metabolic process	47	1.7	5.99E-06	5.22	BP
GO:0006082 organic acid metabolic process	34	1.89	2.56E-05	4.59	BP
GO:0043436 oxoacid metabolic process	33	1.86	5.22E-05	4.28	BP
GO:0006732 coenzyme metabolic process	16	2.58	0.000134	3.87	BP
GO:0044712 single-organism catabolic process	26	1.92	0.000247	3.61	BP
GO:0019752 carboxylic acid metabolic process	31	1.77	0.000272	3.57	BP
GO:0051186 cofactor metabolic process	18	2.2	0.000485	3.31	BP
GO:0006793 phosphorus metabolic process	30	1.74	0.000513	3.29	BP
GO:0090407 organophosphate biosynthetic process	13	2.62	0.000521	3.28	BP
GO:0009056 catabolic process	36	1.6	0.000654	3.18	BP
GO:0044711 single-organism biosynthetic process	26	1.77	0.000989	3	BP
GO:0030307 positive regulation of cell growth	4	6.44	0.001018	2.99	BP
GO:0019637 organophosphate metabolic process	23	1.85	0.001108	2.96	BP
GO:0005739 mitochondrion	36	1.57	0.001023	2.99	CC
GO:0044429 mitochondrial part	27	1.68	0.002021	2.69	CC
GO:0031984 organelle subcompartment	6	3.78	0.002385	2.62	CC
GO:0005759 mitochondrial matrix	18	1.82	0.005261	2.28	CC
GO:0031967 organelle envelope	22	1.69	0.005491	2.26	CC
GO:0031975 envelope	22	1.69	0.005491	2.26	CC
GO:0005740 mitochondrial envelope	18	1.8	0.006059	2.22	CC
GO:0036020 endolysosome membrane	3	6.15	0.00644	2.19	CC
GO:0048037 cofactor binding	16	2.33	0.000503	3.3	MF
GO:0016407 acetyltransferase activity	3	8.16	0.001787	2.75	MF
GO:0050662 coenzyme binding	12	2.39	0.002185	2.66	MF
GO:0016740 transferase activity	19	1.8	0.004585	2.34	MF
GO:0016874 ligase activity	7	3.01	0.004849	2.31	MF
GO:0016853 isomerase activity	6	3.27	0.005771	2.24	MF
GO:0000287 magnesium ion binding	5	3.71	0.0063	2.2	MF
GO:0004497 monooxygenase activity	3	6.12	0.006511	2.19	MF

GO, gene ontology; HSPN, henoch-schönlein purpura nephritis; BP, biological process; CC: cellular component; MF, molecular function.

viral latency. Up-regulated DEPs in the cellular component category (**Figure 4B**) were mostly located in mitochondria and cytoplasm, which were mainly involved in organelle envelope, secretory vesicles and golgi network transport. By contrast, down-regulated DEPs were located in the cytoplasm, which were mainly involved in organelle and cytoskeletal structure. Up-regulated DEPs in the molecular function category (**Figure 4C**) were mainly involved in a variety of enzymes activities, particularly acetyltransferase, and binding of ions. Down-regulated proteins were enriched in guanyl-nucleotide exchange factor activity, cytoskeletal protein binding and phosphatase regulator activity.

For DEPs in the KEGG pathway (**Figure 4D**), up-regulated proteins were involved in butanoate metabolism and adherens junction, and down-regulated proteins were involved in vascular smooth muscle contraction. For DEPs in the protein domain cluster analyses (**Figure 4E**), up-regulated proteins were involved in dehydrogenase and ribosome activity. Down-regulated proteins were involved in the EF-hand domain and FERM domains.

PPI network construction

To better elucidate the protein mechanisms associated with HSPN, STRING and Cytoscape were used to obtain PPI information concerning

Table 2. GO analysis of down-regulated genes associated with HSPN

Term	Count	Fold enrichment	Fisher' exact test *P* value	-log10 (*p* value)	Function
GO:0035303 regulation of dephosphorylation	5	6.78	0.000408	3.39	BP
GO:0006996 organelle organization	24	1.82	0.00053	3.28	BP
GO:0035304 regulation of protein dephosphorylation	4	7.23	0.001265	2.9	BP
GO:0007409 axon genesis	4	7.23	0.001265	2.9	BP
GO:0048812 neuron projection morphogenesis	5	5.42	0.001342	2.87	BP
GO:0048858 cell projection morphogenesis	5	5.08	0.001862	2.73	BP
GO:0097485 neuron projection guidance	3	9.76	0.002001	2.7	BP
GO:0007411 axon guidance	3	9.76	0.002001	2.7	BP
GO:0019219 regulation of nucleobase-containing compound metabolic process	17	1.98	0.002155	2.67	BP
GO:0032990 cell part morphogenesis	5	4.79	0.002516	2.6	BP
GO:0060255 regulation of macromolecule metabolic process	24	1.64	0.002723	2.57	BP
GO:0043170 macromolecule metabolic process	27	1.55	0.002812	2.55	BP
GO:0031032 actomyosin structure organization	4	5.92	0.00302	2.52	BP
GO:0044260 cellular macromolecule metabolic process	23	1.66	0.003174	2.5	BP
GO:0008091 spectrin	3	11.92	0.000898	3.05	CC
GO:0044463 cell projection part	9	2.35	0.010287	1.99	CC
GO:0015630 microtubule cytoskeleton	9	2.35	0.010287	1.99	CC
GO:0005856 cytoskeleton	15	1.7	0.018681	1.73	CC
GO:0005654 nucleoplasm	17	1.61	0.020541	1.69	CC
GO:0005938 cell cortex	6	2.65	0.020734	1.68	CC
GO:1990391 DNA repair complex	2	7.95	0.02145	1.67	CC
GO:0032982 myosin filament	2	7.95	0.02145	1.67	CC
GO:0005085 guanyl-nucleotide exchange factor activity	4	8.08	0.000756	3.12	MF
GO:0008092 cytoskeletal protein binding	13	2.44	0.001184	2.93	MF
GO:0005516 calmodulin binding	5	4.75	0.002599	2.59	MF
GO:0019888 protein phosphatase regulator activity	3	8.08	0.003908	2.41	MF
GO:0019208 phosphatase regulator activity	3	8.08	0.003908	2.41	MF
GO:0005088 Ras guanyl-nucleotide exchange factor activity	3	6.93	0.006541	2.18	MF
GO:0098772 molecular function regulator	10	2.24	0.009219	2.04	MF
GO:0003779 actin binding	8	2.54	0.009818	2.01	MF

GO, gene ontology; HSPN, henoch-schönlein purpura nephritis; BP, biological process; CC: cellular component; MF, molecular function.

identified 149 DEPs. A total of 73 proteins were constructed based on the PPI network, and the majority of DEPs were involved in 2 notable networks (**Figure 5**). One group of proteins was related to adherent junction pathway, including CTNNB1, CDC42, IQGAP1, FN1, ACTN4, ACTB, USO1, PROF1 and NUMA1. The other group of proteins was involved in the mitochondrial beta-oxidation pathway, including EHHADH, ACAT1, HADHA, ACAA2 and HSD17B10.

Validation of cytoskeletal associated protein expressions

Results of the bioinformatics analyses indicated that many up-regulated proteins were enriched in adherens junction pathway. Therefore, the proteins associated with adherens junction, specifically CTNNB1 and CDC42, were selected for validation via immunohistochemistry and real-time PCR assays. Results of these assays demonstrated that both CTNNB1 and CDC42 were significantly up-expressed in HSPN patients (**Figure 6**).

Discussion

Although it has been well established that HSPN mainly results from glomerular deposition of IgA-CIC, there remains much to be understood regarding the complex molecular mechanisms involved in the cascade of cross-talk between resident cells and inflammatory cells [15]. Most of the works in this area have been focused on the analyses of clinical manifestations and urine samples, in which animal models were used [16, 17], while direct studies involving renal biopsy are quite rare. In this study, we directly examined changes in protein levels using quantitative proteomics, and then

Table 3. KEGG analysis of DEPs associated with HSPN

Regulation	ID	Term	Count	Fold enrichment	-log10 (*p* value)	Genes
Up-regulated	hsa00650	Butanoate metabolism	6	3.61	2.62	OXCT1, ACSM2A, EHHADH, ACAT1, ABAT, HADHA
Up-regulated	hsa00410	beta-Alanine metabolism	6	3.06	2.16	EHHADH, ABAT, ALDH6A1, ALDH2, HADHA, CNDP2
Up-regulated	hsa04520	Adherens junction	4	3.78	1.93	IQGAP1, CDC42, ACTB, ACTN4
Up-regulated	hsa00520	Amino sugar and nucleotide sugar metabolism	3	4.97	1.93	HEXB, PGM1, CYB5R3
Up-regulated	hsa00640	Propanoate metabolism	6	2.48	1.65	EHHADH, ACAT1, ABAT, ALDH6A1, HADHA, SUCLG2
Up-regulated	hsa00380	Tryptophan metabolism	5	2.55	1.48	EHHADH, ACAT1, OGDH, ALDH2, HADHA
Up-regulated	hsa01200	Carbon metabolism	12	1.66	1.38	TPI1, EHHADH, ACAT1, GAPDH, OGDH, HADHA, TKT ACO1, GOT2, ALDH6A1, PKM, SUCLG2
Up-regulated	hsa00280	Valine, leucine and isoleucine degradation	8	1.89	1.34	OXCT1, EHHADH, ACAT1, ABAT, HSD17B10, ALDH6A1, ALDH2, HADHA
Down-regulated	hsa04270	Vascular smooth muscle contraction	3	6.12	2	CALM1, MYH10, MYH11

KEGG, Kyoto Encyclopedia of Genes and Genomes; HSPN, henoch-schönlein purpura nephritis; DEPs, differentially expressed proteins.

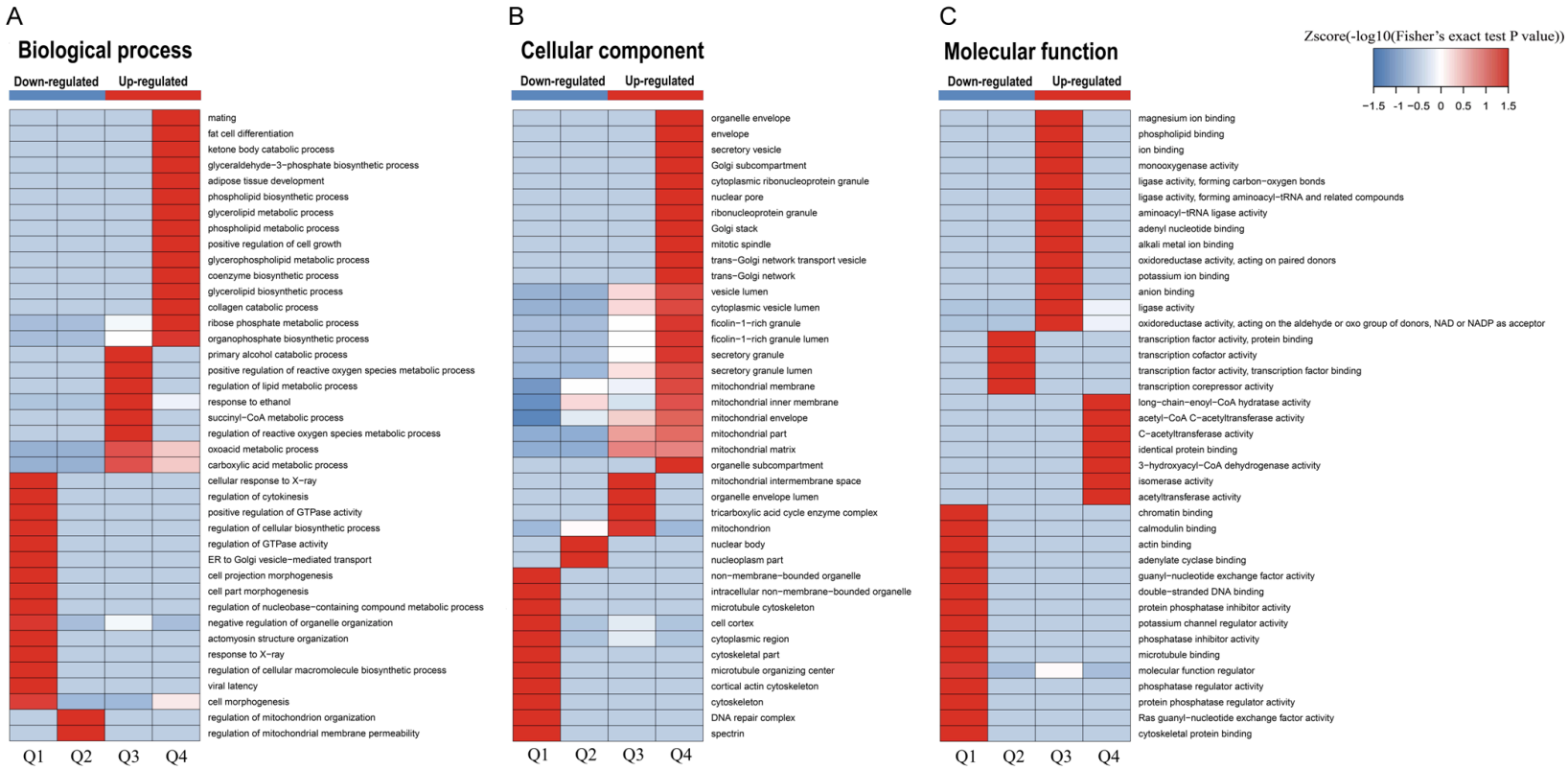

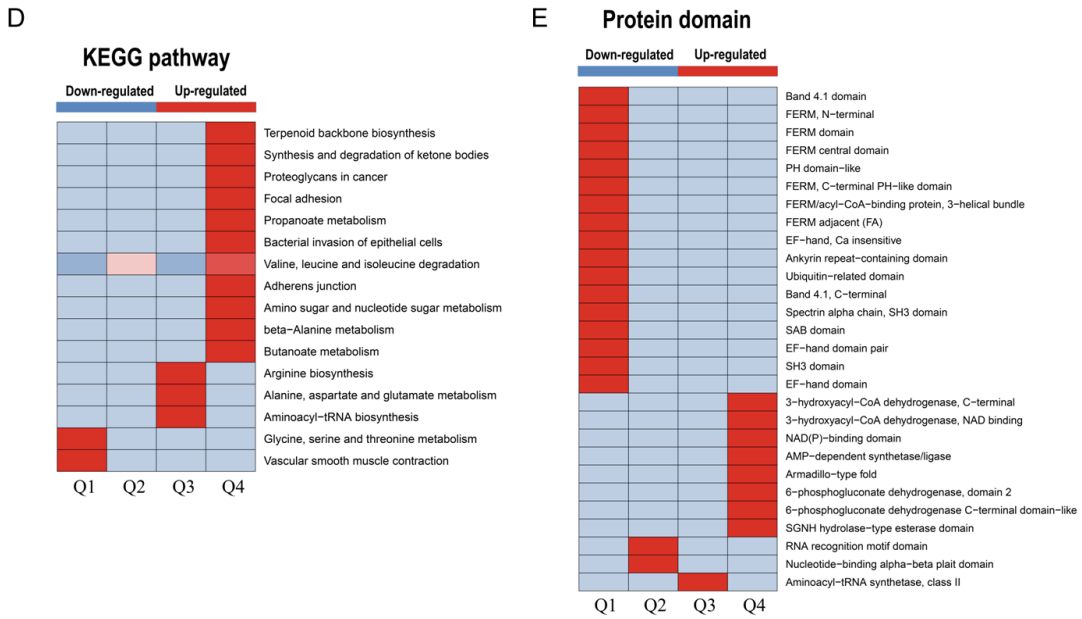

Figure 4. Functional enrichment-based hierarchical clustering analysis of the DEPs. A. Biological process. B. Cellular component. C. Molecular function. D. KEGG pathway. E. Protein domain. The horizontal axis represents the groups of DEPS according to the ratios of differential expression (Q1: 0 < Ratio ≤ 1/4, Q2: 1/4 < Ratio ≤ 1/2, Q3: 2 < Ratio ≤ 4, Q4: Ratio > 4). The vertical axis represents the name of term in the different functional enrichments. The color denotes the degree of enrichment (Z score) of each block with red signifying higher levels of enrichment and blue lower levels. DEPs, differently expressed proteins; KEGG, Kyoto Encyclopedia of Genes and Genomes.

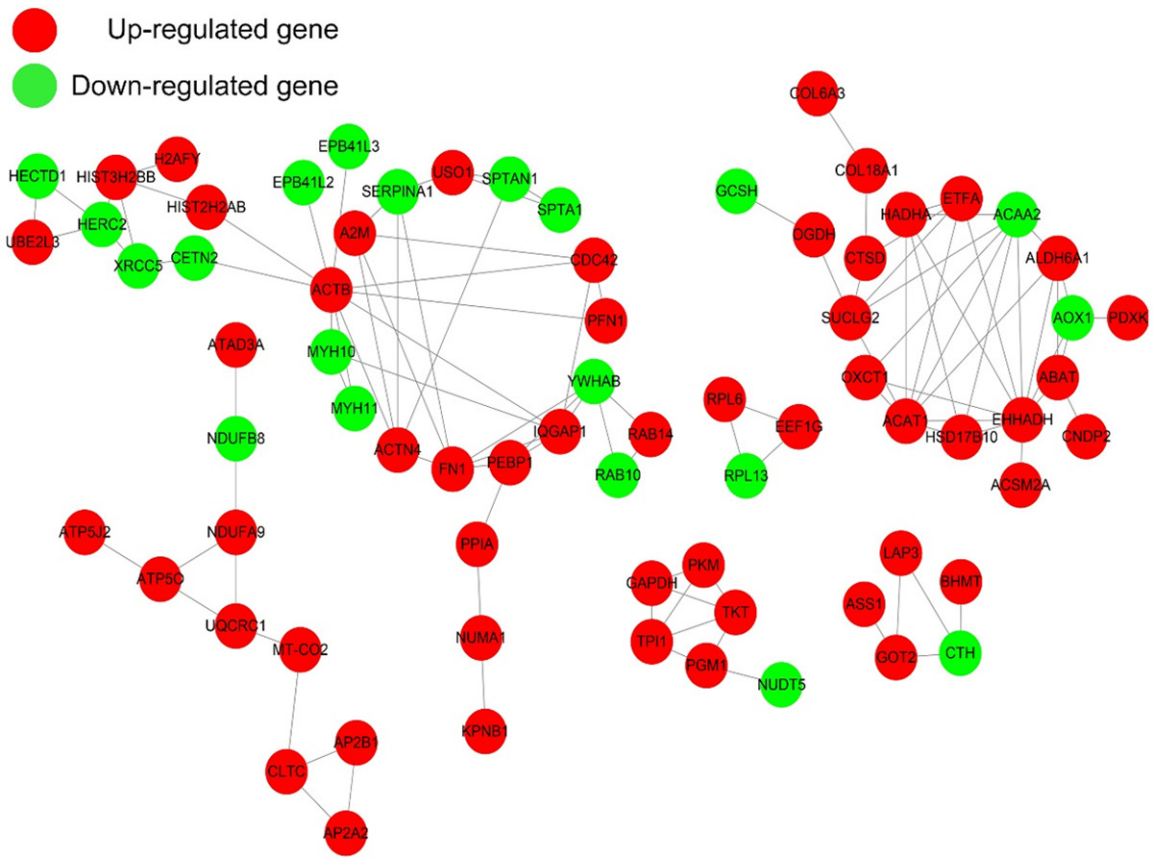

Figure 5. Protein-protein interactions of DEPs. The PPI network was constructed and formatted with up-regulated proteins shown in red circles and down-regulated proteins in green circles. Straight lines connecting circle edges indicate protein-protein interactions. PPI, protein-protein interaction.

combined these findings with those of LC-MS/MS analyses to identify pivotal molecules and signal pathways involved in HSPN.

The DEPs identified in the renal tissue of HSPN patients consisted of 97 up-regulated and 52 down-regulated proteins.

Kidneys are a major organ of the body for the clearance of many metabolites and play a vital role in maintaining electrolyte levels, and composition of blood, and are also responsible for substance metabolism processes and metabolizing enzymes [18]. In the present study, the GO and KEGG enrichment analyses revealed that up-regulated proteins were mainly related to metabolism and adherens junction. In terms of metabolism, DEPs were mainly enriched in lipid metabolism and butanoate metabolism. HADHA, a protein of the butanoate metabolism pathway, is involved in the reactions in the mitochondrial β-oxidation pathway, which is a main energy-producing process in tissues for breaking down fatty acids into acetyl-CoA units [19]. It has been reported that disorders of lipid metabolism exacerbate chronic kidney disease [20]. While renal dysfunction may lead to perturbation in lipoprotein metabolism, lipoprotein abnormalities accelerate the rate of progression of renal dysfunction [21]. Although no direct evidence suggests that lipid metabolism is associated with HSPN, the fact that HSPN is a multifactorial disease indicates that lipid metabolic disorders may participate in the pathogenesis of this condition.

The functional enrichment analysis showed that up-regulated DEPs also have a close relationship with adherens junction. The KEGG enrichment analysis revealed that four DEPs were involved in adherens junction pathway, including actin, F-actin, CDC42 and IQGAP1. All four proteins were involved in regulating the cytoskeleton function of podocytes. Actin cyto-

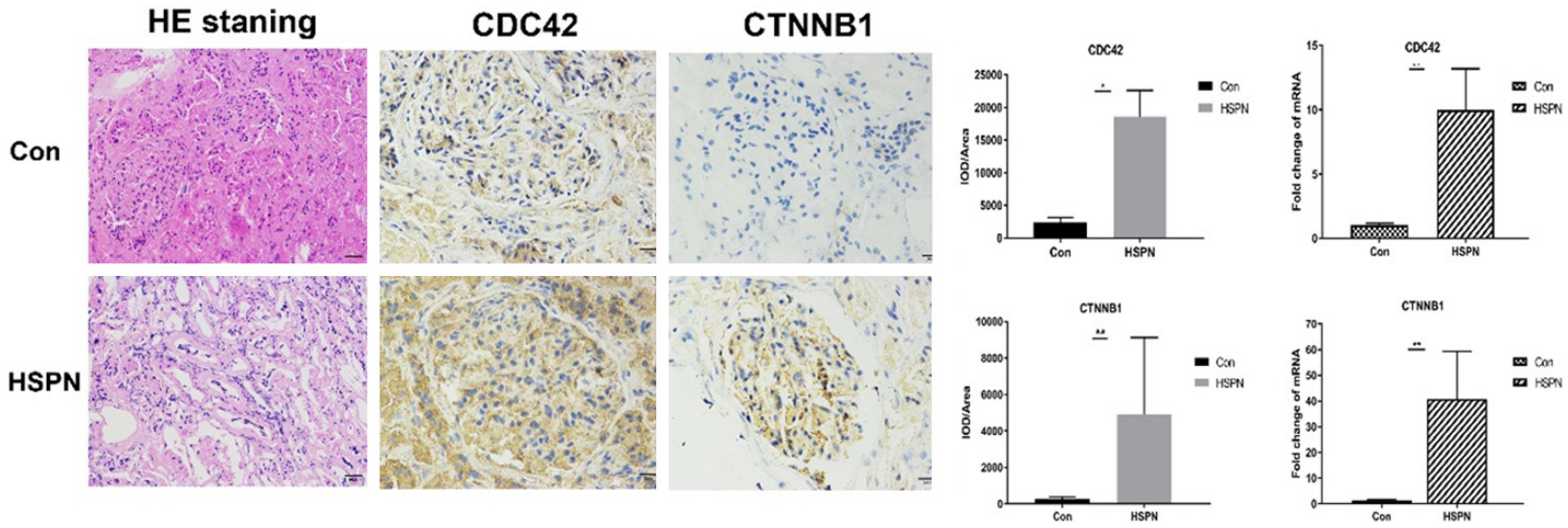

Figure 6. Analysis of pathological changes of glomeruli and validation selected differentially expressed proteins. Significant necrosis and infiltration of inflammatory cells were observed in the glomeruli of HSPN patients (hematoxylin and eosin × 200). CDC42 and CTNNB1, were detected with use of immunohistochemistry and real-time PCR. The protein and mRNA expressions of CDC42 and CTNNB1 were both increased in HSPN patients as compared with healthy controls. Data are presented as means ± SDs. * and ** indicate $P < 0.05$ and $P < 0.01$.

skeleton is an essential structural and functional element involved in controlling podocytes activity, while a variety of actin-associated proteins can regulate actin cytoskeletal dynamics, cell adhesive interactions and motility [22]. As an actin-associated protein, CDC42 is known to be not only a powerful regulator of actin cytoskeletal dynamics, but also related to the pathogenesis of kidney disease progression [23], and the deletion of CDC42 will cause congenital nephrotic syndrome, podocyte foot process effacement and glomerulosclerosis [24, 25]. With regard to IQGAP1, this protein has been reported to be involved in actin cytoskeleton organization and regulation of podocyte function [26]. Consistent with the findings of this proteomics analysis, we found that the CDC42 and CTNNB1 proteins and mRNA were markedly up-expressed in renal samples from HSPN patients as compared to healthy controls. CTNNB1 is considered to play a pivotal role in promoting podocyte injury via Wnt/β-catenin signaling and it has been well established that Wnt/β-catenin signaling consistently aggravates podocyte injury and proteinuria, which leads to the involvement of other pathways in mediating podocytopathy [27]. The increased expression of adherent junction pathway associated proteins suggests that abnormalities in cell junctions are likely linked to the pathogenesis of HSPN, especially with regard to their capacity to injure podocytes.

Results of the PPI network analysis were consistent with those of the functional enrichment analysis, both of them indicated that many proteins were involved in adherent junctions and lipid metabolism, including CTNNB1, CDC42, IQGAP1, FN1, ACTB, USO1, PROF1, NUMA1, EHHADH, ACAT1, HADHA, ACAA2 and HSD-17B10.

Up-regulation of CNDP2 and ACTN4 might be involved in injuries of podocytes and glomerular filtration membranes. Carnosinase, an enzyme encoded by CNDP1 and CNDP2, has been reported to play a renal protective role as a scavenger of reactive oxygen species. Ahluwalia et al, reported that a single nucleotide polymorphisms (SNP) of CNDP2 was associated with an increased risk of diabetic nephropathy as indicated by increased albumin excretion and decreased glomerular filtration rates [28]. ACTN4 encodes the protein α-actinin 4, which exerts a significant effect in maintaining the renal filtration barrier [29]. In the study of Henderson et al, it was found that ACTN4 mutations resulted in podocyte injuries, which were associated with renal dysfunctions such as familial focal segmental glomerulosclerosis (FSGS) [30]. Currently there is no direct evidence that demonstrates a relationship of CNDP2 and ACTN4 with HSPN, but it was observed that these two proteins were significantly increased in renal tissues of these HSPN patients, which suggests that SNP and mutations may also be involved in the pathogenesis of HSPN.

The down-regulated proteins, such as CALM1, MYH10 and MYH11 are enriched in the vascular smooth muscle contraction pathway. CALM encodes calmodulin, which is essential for Ca^{2+} dependent cellular events [31]. As kidney diseases can result in marked alterations of metabolic activity [32], the down-regulation of CALM may be related to Ca^{2+} signal transduction disorder. MYH10 and MYH11 encode major myosin II motor proteins and myosin heavy chain 11 proteins respectively. MYH10 is a cytoskeletal protein with diverse functions including cytokinesis and regulation of cell shape, adhesion and migration. In kidney development, a mutation in MYH10 can result in end-stage renal failure in the adult. In addition, MYH10 affects coronary vessel development, and our PPI network and KEGG analyses revealed that MYH10 and MYH11 were associated with vascular smooth muscle contraction [33]. Therefore, renal vessel development may also be compromised by mutations in these proteins. In this study, the proteomics analysis also indicated that DEPs were implicated in lipid metabolism and adherent junction pathways, which might be involved in the pathophysiological mechanisms of HSPN. This validation further demonstrated that the adherent junction associated proteins, such as CDC42 and CTNNB1, were increased in renal tissues of HSPN patients as compared with those of healthy controls.

For all we know, this is the first attempt to determine HSPN-associated molecules and signal pathways in renal tissues of HSPN patients. While it is important to note that these analyses of renal tissue samples are limited to the constraints of the iTRAQ technique, 149 DEPs

detected in this study provide a solid foundation for future bioinformatic analyses.

In conclusion, the DEPs detected in this study are mostly enriched in lipid metabolism and adherent junction pathways. Such processes can affect the progression of kidney disease, particularly with regard to the regulation of podocyte functions. This study enables us to identify some of the biological processes and signal pathways demonstrating remarkable changes as related to HSPN, but the exact roles and mechanisms of these functions as related to HSPN remain to be studied.

Acknowledgements

The work was supported by natural science foundation of Liaoning Province, China (grant no. 20170540538).

Disclosure of conflict of interest

None.

Address correspondence to: Dr. Liang He, Department of Thyroid Surgery, No. 1 Hospital of China Medical University, 155N Nanjing Street, Heping, Shenyang 110001, Liaoning, China. E-mail: hl_31@163.com

References

[1] Santos FM, Gaspar LM, Ciordia S, Rocha AS, Castro E Sousa JP, Paradela A, Passarinha LA and Tomaz CT. iTRAQ quantitative proteomic analysis of vitreous from patients with retinal detachment. Int J Mol Sci 2018; 19: 1-22.

[2] Pillebout E, Jamin A, Ayari H, Housset P, Pierre M, Sauvaget V, Viglietti D, Deschenes G, Monteiro RC and Berthelot L; HSPrognosis group. Biomarkers of IgA vasculitis nephritis in children. PLoS One 2017; 12: e0188718.

[3] Roache-Robinson P and Hotwagner DT. Henoch Schonlein Purpura (Anaphylactoid Purpura, HSP). StatPearls. Treasure Island (FL): 2019.

[4] Jelusic M, Sestan M, Cimaz R and Ozen S. Different histological classifications for Henoch-Schonlein purpura nephritis: which one should be used? Pediatr Rheumatol Online J 2019; 17: 1-7.

[5] Narchi H. Risk of long term renal impairment and duration of follow up recommended for Henoch-Schonlein purpura with normal or minimal urinary findings: a systematic review. Arch Dis Child 2005; 90: 916-920.

[6] Wakaki H, Ishikura K, Hataya H, Hamasaki Y, Sakai T, Yata N, Kaneko T and Honda M. Henoch-schonlein purpura nephritis with nephrotic state in children: predictors of poor outcomes. Pediatr Nephrol 2011; 26: 921-925.

[7] Huang X, Wu X, Le W, Hao Y, Wu J, Zeng C, Liu Z and Tang Z. Renal prognosis and related risk factors for henoch-schonlein purpura nephritis: a Chinese adult patient cohort. Sci Rep 2018; 8: 5585-5592.

[8] Kanaan N, Mourad G, Thervet E, Peeters P, Hourmant M, Vanrenterghem Y, De Meyer M, Mourad M, Marechal C, Goffin E and Pirson Y. Recurrence and graft loss after kidney transplantation for henoch-schonlein purpura nephritis: a multicenter analysis. Clin J Am Soc Nephrol 2011; 6: 1768-1772.

[9] Pohl M. Henoch-schonlein purpura nephritis. Pediatr Nephrol 2015; 30: 245-252.

[10] Berthelot L, Papista C, Maciel TT, Biarnes-Pelicot M, Tissandie E, Wang PH, Tamouza H, Jamin A, Bex-Coudrat J, Gestin A, Boumediene A, Arcos-Fajardo M, England P, Pillebout E, Walker F, Daugas E, Vrtosvnik F, Flamant M, Benhamou M, Cogne M, Moura IC and Monteiro RC. Transglutaminase is essential for IgA nephropathy development acting through IgA receptors. J Exp Med 2012; 209: 793-806.

[11] Heineke MH, Ballering AV, Jamin A, Ben Mkaddem S, Monteiro RC and Van Egmond M. New insights in the pathogenesis of immunoglobulin A vasculitis (Henoch-schonlein purpura). Autoimmun Rev 2017; 16: 1246-1253.

[12] Li H, Han J, Pan J, Liu T, Parker CE and Borchers CH. Current trends in quantitative proteomics - an update. J Mass Spectrom 2017; 52: 319-341.

[13] Guan W, Liu Y, Li X, Yang B and Kuang H. iTRAQ-based proteomics to reveal the mechanism of hypothalamus in kidney-yin deficiency rats induced by levothyroxine. Evid Based Complement Alternat Med 2019; 2019: 3703596.

[14] Persson F and Rossing P. Urinary proteomics and precision medicine for chronic kidney disease: current status and future perspectives. Proteomics Clin Appl 2019; 13: e1800176.

[15] Davin JC and Coppo R. Henoch-schonlein purpura nephritis in children. Nat Rev Nephrol 2014; 10: 563-573.

[16] Su S, Yu J, Wang Y, Wang Y, Li J and Xu Z. Clinicopathologic correlations of renal biopsy findings from northeast China: a 10-year retrospective study. Medicine (Baltimore) 2019; 98: e15880.

[17] Suzuki H and Suzuki Y. Murine models of human IgA nephropathy. Semin Nephrol 2018; 38: 513-520.

[18] Bajaj P, Chowdhury SK, Yucha R, Kelly EJ and Xiao G. Emerging kidney models to investigate metabolism, transport, and toxicity of drugs and xenobiotics. Drug Metab Dispos 2018; 46: 1692-1702.
[19] Spencer NY and Stanton RC. Glucose 6-phosphate dehydrogenase and the kidney. Curr Opin Nephrol Hypertens 2017; 26: 43-49.
[20] Chen DQ, Chen H, Chen L, Vaziri ND, Wang M, Li XR and Zhao YY. The link between phenotype and fatty acid metabolism in advanced chronic kidney disease. Nephrol Dial Transplant 2017; 32: 1154-1166.
[21] Bulbul MC, Dagel T, Afsar B, Ulusu NN, Kuwabara M, Covic A and Kanbay M. Disorders of lipid metabolism in chronic kidney disease. Blood Purif 2018; 46: 144-152.
[22] Zigmond SH. Signal transduction and actin filament organization. Curr Opin Cell Biol 1996; 8: 66-73.
[23] Huang Z, Zhang L, Chen Y, Zhang H, Zhang Q, Li R, Ma J, Li Z, Yu C, Lai Y, Lin T, Zhao X, Zhang B, Ye Z, Liu S, Wang W, Liang X, Liao R and Shi W. Cdc42 deficiency induces podocyte apoptosis by inhibiting the Nwasp/stress fibers/YAP pathway. Cell Death Dis 2016; 7: e2142.
[24] Scott RP, Hawley SP, Ruston J, Du J, Brakebusch C, Jones N and Pawson T. Podocyte-specific loss of Cdc42 leads to congenital nephropathy. J Am Soc Nephrol 2012; 23: 1149-1154.
[25] Blattner SM, Hodgin JB, Nishio M, Wylie SA, Saha J, Soofi AA, Vining C, Randolph A, Herbach N, Wanke R, Atkins KB, Gyung Kang H, Henger A, Brakebusch C, Holzman LB and Kretzler M. Divergent functions of the Rho GTPases Rac1 and Cdc42 in podocyte injury. Kidney Int 2013; 84: 920-930.
[26] Li Z, McNulty DE, Marler KJ, Lim L, Hall C, Annan RS and Sacks DB. IQGAP1 promotes neurite outgrowth in a phosphorylation-dependent manner. J Biol Chem 2005; 280: 13871-13878.
[27] Zhou L and Liu Y. Wnt/beta-catenin signalling and podocyte dysfunction in proteinuric kidney disease. Nat Rev Nephrol 2015; 11: 535-545.
[28] Ahluwalia TS, Lindholm E and Groop LC. Common variants in CNDP1 and CNDP2, and risk of nephropathy in type 2 diabetes. Diabetologia 2011; 54: 2295-2302.
[29] Meng L, Cao S, Lin N, Zhao J, Cai X, Liang Y, Huang K, Lin M, Chen X, Li D, Wang J, Yang L, Wei A, Li G, Lu Q, Guo Y, Wei Q, Tan J, Huang M, Huang Y, Wang J and Liu Y. Identification of a novel ACTN4 gene mutation which is resistant to primary nephrotic syndrome therapy. Biomed Res Int 2019; 2019: 5949485.
[30] Henderson JM, Alexander MP and Pollak MR. Patients with ACTN4 mutations demonstrate distinctive features of glomerular injury. J Am Soc Nephrol 2009; 20: 961-968.
[31] Rocchetti M, Sala L, Dreizehnter L, Crotti L, Sinnecker D, Mura M, Pane LS, Altomare C, Torre E, Mostacciuolo G, Severi S, Porta A, De Ferrari GM, George AL Jr, Schwartz PJ, Gnecchi M, Moretti A and Zaza A. Elucidating arrhythmogenic mechanisms of long-QT syndrome CALM1-F142L mutation in patient-specific induced pluripotent stem cell-derived cardiomyocytes. Cardiovasc Res 2017; 113: 531-541.
[32] Pawelczyk T, Easom RA and Olson MS. The effects of various anions and cations on the regulation of pyruvate dehydrogenase complex activity from pig kidney cortex. Biochem J 1988; 253: 819-825.
[33] Haque F, Kaku Y, Fujimura S, Ohmori T, Adelstein RS and Nishinakamura R. Non-muscle myosin II deletion in the developing kidney causes ureter-bladder misconnection and apical extrusion of the nephric duct lineage epithelia. Dev Biol 2017; 427: 121-130.